Bull. Mar. Res. Inst.
Cheju Nat. Univ., 16 : 1~13, 1992

濟州大 海洋硏報 16 : 1~13, 1992

Theory of Forced Shelf Waves over a Double Shelf

Ig-Chan Pang · Tae-Hee Kim

Dept. of Oceanography, College of Ocean Science, Cheju National University, Cheju 690-756, Korea

양향성 대륙붕에서의 강제파이론

방 익 찬 · 김 태 희

제주대학교 해양과학대학 해양학과

The first order wave equation over a double shelf has wind stresses on both coastal boundaries and wind stress curl forcing across the shelf. In the Yellow Sea, the effect of wind stress curl can be neglected as a forcing of shelf waves. The decay distance of Kelvin waves are much greater than that of continental shelf waves so that Kelvin waves are transmitted nearly intact through the northern embayment. The numerical method of characteristics has been modified to accomodate wave propagation of opposite directions.

The Kelvin wave makes a substantial contribution to sea level fluctuations. However, it contributes almost nothing to alongshore velocity. Velocity is due mainly to the presence of continental shelf waves, among which the 1st modes contribute the most.

Key words : 대륙붕파(continental shelf wave), 켈빈파(kelvin wave), 양향성 대륙붕(double shelf)

Introduction

The theory of coastally trapped waves over a double shlf topography shown in the Yellow Sea has been recently studied, and based on the theory, a long wave model has been developed and applied to the Yellow Sea to reproduce sea level and velocity fluctuations during January to March 1986 (Pang, 1987; Hsueh and Pang, 1989). The application has been successful, specially in reproducing qualitatively the upwind flow bursts in the Yellow Sea trough. The success make the model to be used to address the dynamices of the Yellow Sea circulation. However, more processes should be added to develop the theory and the wave model. Some of them have been worked for free waves in Pang (1991, 1992) and some of them are going to be worked for forced waves in this study.

A forced wave equation in frictionless case is first derived by Gill and Schumann (1974) for a single shelf and friction is added incurring an infinite coupled set of modes by Brink and Allen (1978). The fully coupled set of wave equations is first solved by integration along the characteristics by Clarke and VanGorder (1986). The wave equation for a double shelf is derived and solved by Pang (1987).

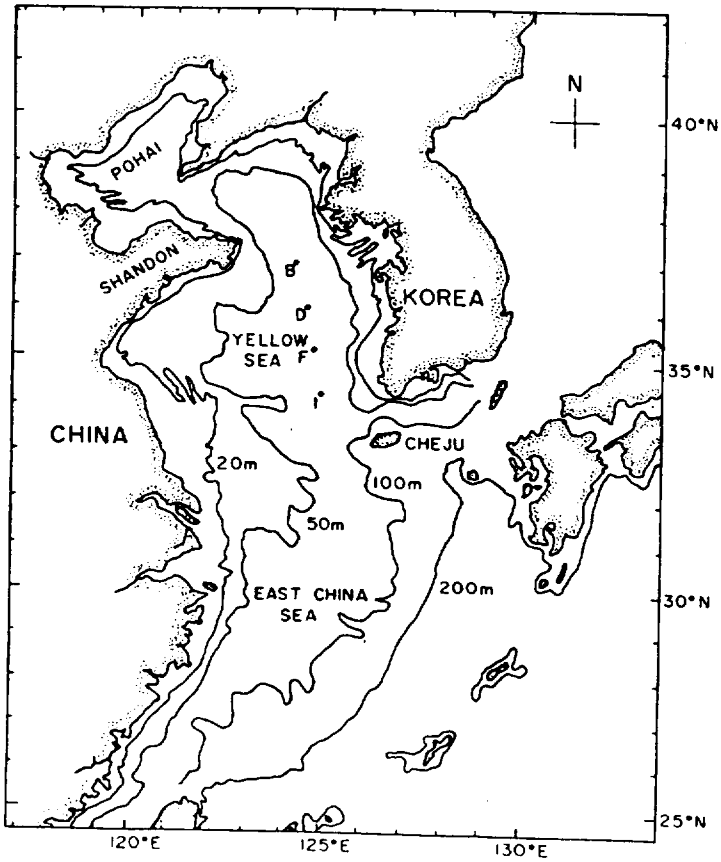

Fig. 1. Map of the Yellow Sea. Depths are in meters. Dots mark the locations of observation for the period of January 10 to April 12, 1986.

The method of characteristics used to solve it is basically similar to that found in Clarke and VanGorder (1986), except that the integration proceeds in time increment to accomodate wave propagation to the north and south (Clarke and VanGorder used a distance increment, which is possible for only one-directional wave propagation.) and that for a given resolution in y, time increment is much smaller that Kelvin waves are included (Kelvin wave is not included in most previous shlf wave models.).

We have chosen the Yellow Sea to examine a double shelf system. Fig. 1 shows the bottom topography of the Yellow Sea and the locations of observation. The Yellow Sea is essentially a north-south running shallow channel with a double shelf cross section. The study of long waves in semienclosed channels with flat bottoms dates back to the early 1900s (Taylor, 1921). In the late 1990s, long waves have been studied over bottom porfiles characterized by a reversal slope encountered across submarine banks and trenches (Louis, 1978; Mysak et al. 1979; Mysak, 1980; Mysak and Willmott, 1981; Brink, 1983). However, the addition of Kelvin waves renders the circumstances in the Yellow Sea different. The purpose of the present study is to develop the existing basic theory for forced shelf waves over a double shelf.

The Process of Theory

The process by which the wave model has been made is shown in Fig. 2. First step is to solve the free problem, in which bottom topography is incorporated. We have obtained the dispersion relation, from which the eigenvalues C_n (phase speeds here) are calculated, and eigenfunctions F_n for a double shelf as shown in the Yellow Sea. In the next forced problem the first order wave equation is derived for a double shelf. By integration of wave equation, the wave function ϕ_n is solved. Geometry, frictional effect, and wind stress are incorporated in the wave equation. Finally, the eigenfunctions and wave functions are combined to get the sea level and velocity.

First Order Wave Equation

For long shelf wave motions influenced by winds, small perturbations to a barotropic ocean satisfy the equation.

$$(HP_{xt})_x + (rP_x)_x - fH_xP_y - \frac{f^2}{g}P_t = f(\tau^y_x - \tau^x_y) \quad (1)$$

In this equation, x, y, t, p, g, f, r, H, τ^x and τ^y refer respectively to cross-shelf distance (eastward positive), alongshore distance (northward positive), time, perturbation pressure divided by mean water

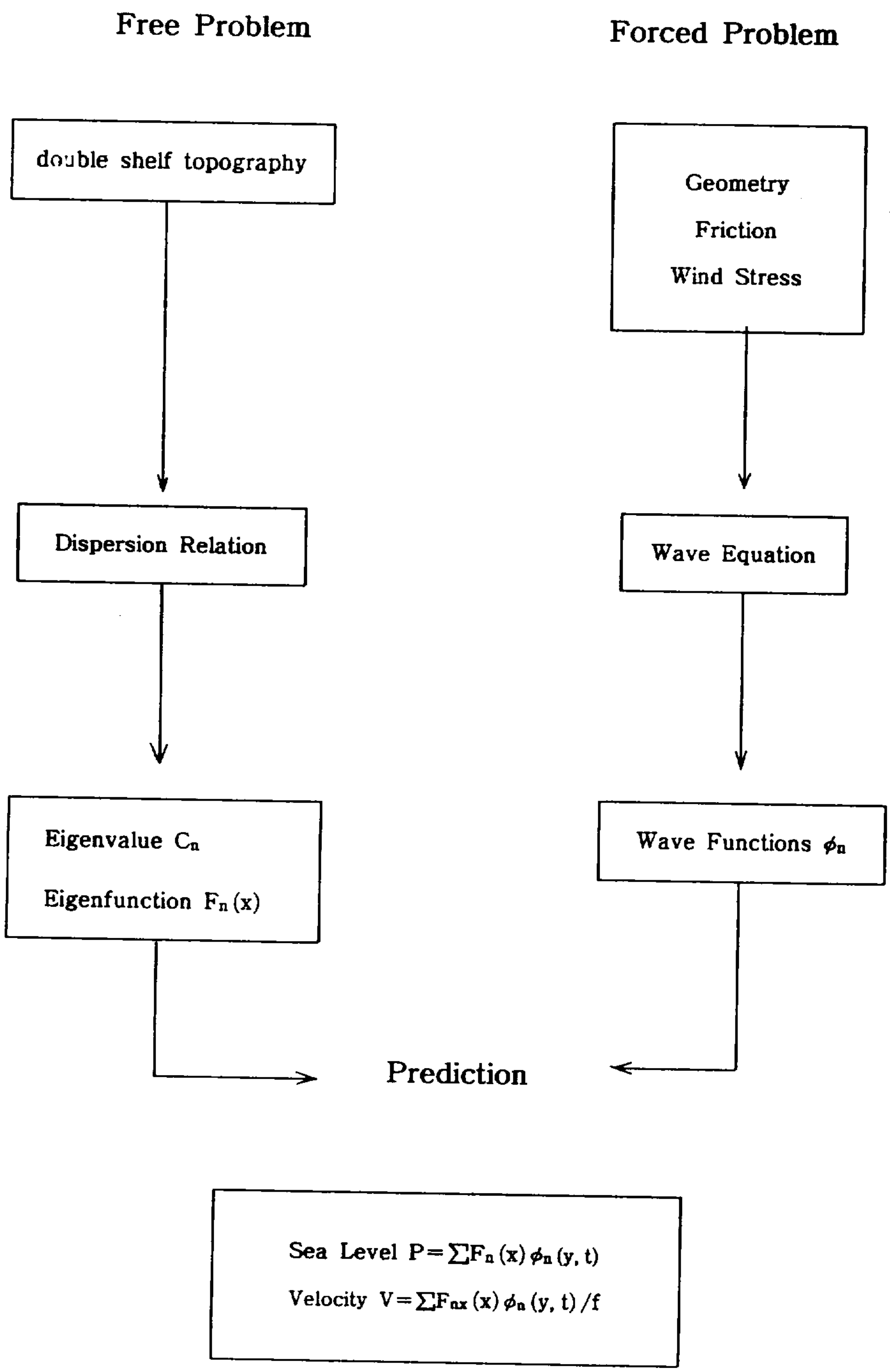

Fig. 2 Chart of the processes by which the wave model is made

density, acceleration due to gravity, Coriolis parameter, bottom resistance coefficient, water depth, kinematic wind stresses in x and y direction at surface (the wind stresses divided by mean water density). Subscripts indicate derivatives.

Fig. 3 shows a schematic representation of the coordinates system and geometry of double shelves of linear depth profile, which is adapted for the Yellow Sea. The coordinates z refers to the vertical distancd (upward positive). The origin of coordinates is set at the sea surface on the intersection of the trough and southern boundary. Shelf 1 and shelf 2 are placed in $-B_1 \leq x \leq 0$ and $0 \leq x \leq B_2$, respectively. So, the linear bottom topography (H) can be set as follows :

$$H(X) = \begin{cases} H_1 = H_o \dfrac{x+L_1}{L_1} & -B_1 \leq x \leq 0 \\ \quad \text{in shelf 1 (China shelf)} & \\ H_2 = -H_o \dfrac{x-L_2}{L_2} & -0 \leq x \leq B_2 \\ \quad \text{in shelf 2 (Korea shelf)} & \end{cases} \quad (2)$$

At the coastal boundaries, the no-flux boundary condition is applied, which means that the depth integrated offshore velocity vanishes (Pang, 1991, 1992). At the boundary between two shelves, the continuous boundary conditions of pressure and transverse velocity are applied, as follows :

$$P_{1xt} + \frac{r}{h} p_{1x} + fP_{1y} = f\frac{y}{h} \qquad \text{at } x=-B_1 \quad (3\text{-}1)$$

$$P_1 = P_2 \qquad \text{at } x=0 \quad (3\text{-}2)$$

$$P_{1xt} + fP_{1y} = P_{2xt} + fP_{2y} \qquad \text{at } x=0 \quad (3\text{-}3)$$

$$P_{2xt} + \frac{r}{h} p_{2x} + fP_{2y} = f\frac{y}{h} \qquad \text{at } x=B_2 \quad (3\text{-}6)$$

Setting $P(x, y, t) = \sum F_n(x)\phi(y, t)$ yields a Sturm-Louville problem for frictionless eigenfunctions $F_n(x)$ as follows :

$$(HF_{nx})_x + \frac{f}{C_n} H_x F_n - \frac{f^2}{g} F_n = 0 \quad (4)$$

$$F_{1nx} + \frac{f}{c_n} f_{1n} = 0 \qquad \text{at } x=-B_1 \quad (5\text{-}1)$$

$$F_{1n} = F_{2n} \qquad \text{at } x=0 \quad (5\text{-}2)$$

$$F_{1nx} = F_{2nx} \qquad \text{at } x=0 \quad (5\text{-}3)$$

$$F_{2nx} + \frac{f}{c_n} f_{2n} = 0 \qquad \text{at } x=B_2 \quad (5\text{-}4)$$

where F_{1n}:, F_{2n}, c_n are eigenfunctions in shelves 1 and 2, the phase speed of nth mode, respectively.

Multiplying (1) by F_n and (4) by P_t and substracting them yields

$$F_n(HP_{xt})_x - P_t(HF_{nx})_x + (rP_x)_x F_n + fH_x F_n (P_y - \frac{P_t}{C_n}) = fF_n(\tau_x^y - \tau_y^x) \quad (6)$$

By integrating (6) from $-B_1$ to B_2 with the boundary conditions (2) and (5), and expanding the pressure in terms of inviscid eigenfunctions with the orthogonality condition (Pang, 1992), it follows that, for mode n,

$$-\frac{\phi_{nt}}{C_n} + \phi_{ny} + \sum_{m=-\infty}^{\infty} a_{mn}\phi_m = b_{1n} \cdot \tau^y(-B_1) - b_{2n} \cdot \tau^y(B_2) - \frac{1}{r_n}\int_{-B_1}^{B_2} F_n \cdot (\tau_x^y - \tau_y^x)\,dx \quad (7)$$

where

$$a_{mn} = \frac{1}{f \cdot r_n}\left[(-r \cdot F_{mx} \cdot F_n)\Big|_{-B_1}^{B_2} + \int_{-B_1}^{B_2} (r \cdot F_{mx})_x \cdot F_n\,dx\right] \quad (8\text{-}1)$$

$$b_{1n} = \frac{F_n(-B_1)}{r_n} \quad (8\text{-}2)$$

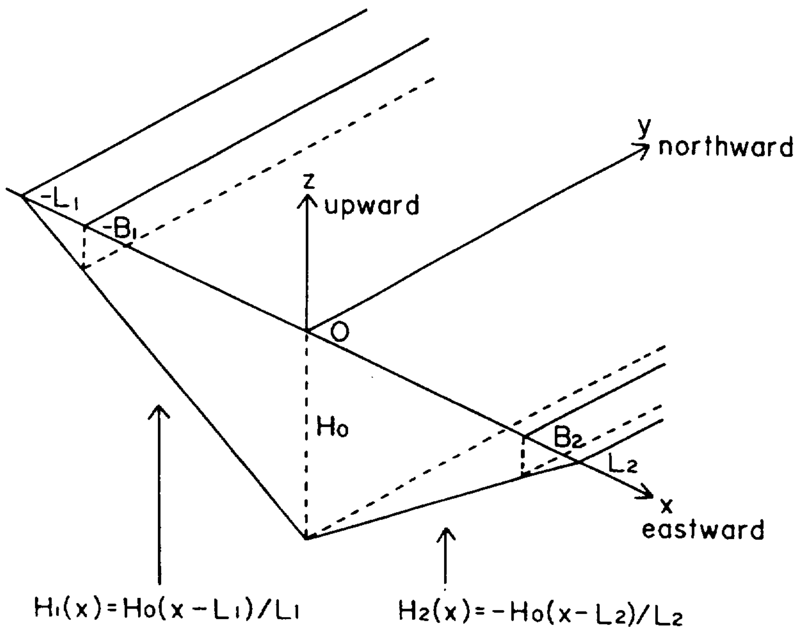

Fig. 3. Schematic representation of the coordinate system and the double shelf topography, which represents the Yellow Sea. The coordinates x, y, and z refer to the cross-shelf (eastward positive), alongshore (northward positive), and vertical directions (upward positive), respectively. The greatest water depth is H_0. B_1 and B_2 are the the locations of no-flux boundary where the water depth is 3 times the Ekman layer thickness (Mitchum and Clarke, 1986).

$$b_{2n}=\frac{F_n(B_2)}{r_n} \tag{8-3}$$

$$r_n=(-H\cdot F_n^2)\Big|_{-B_1}^{B_2}+\int_{-B_1}^{B_2}H_x\cdot F_n^2\,dx \tag{8-4}$$

F_n's and ϕ_n's satisfy the boundary conditions and an infinite set of coupled first order wave equations, respectively. b_{1n} and b_{2n} are, respectively, wind-coupling coefficients at $x=-B_1$ and B_2. a_{nn} is a frictional decay coefficient and a_{mn} is a frictional coupling coefficient to mode m. The wave functions are coupled through friction. If there is no friction $(r=0)$, $a_{mn}=0$ and the modes are decoupled. The reciprocal of $|a_{nn}|$ gives the decay distance for amplitude of the nth wave mode in the direction of wave propagation. For $r=3\times10^{-4}$ m/sec, China shelf with $B_1=300$km, Korea shelf with $B_2=120$km, the trough depth $H_0=100$m, coastal depth=20m, the decay distance of Kelvin wave is O(10,000km) and that of the lst continental shelf wave mode is O(100km). Equation (7) can be solved using the method of characteristics.

As shown in Pang (1991, 1992), there are two infinite sets of wave mode over a double shelf topography. We will use the positive (negative) n for the set of postive (negative) phase speed, which propagate southward (northward) along shelf 1 (2). For the Yellow Sea, the former (latter) will be called Korea (China) waves. The first modes (n=1, -1) are Kelvin waves and the other modes are continental shelf waves.

The first order wave equation (7) over a double shelf has wind stresses on both coastal boundaries and wind stress curl forcing across the shelf. Figure 4 presents the comparison of the wind stress curl term wind stress term. In calculating the wind stress curl, F_n is taken to be unity, representing the normalized value at coast, so that the wind stress curl term is over-estimated. By comparing, the wind stress curl is negligible except at a couple of times when the wind stress curl term shows a spike. The spikes are few in number. Thus, the effect of wind stress curl can be neglected as a forcing of shelf waves in the Yellow Sea.

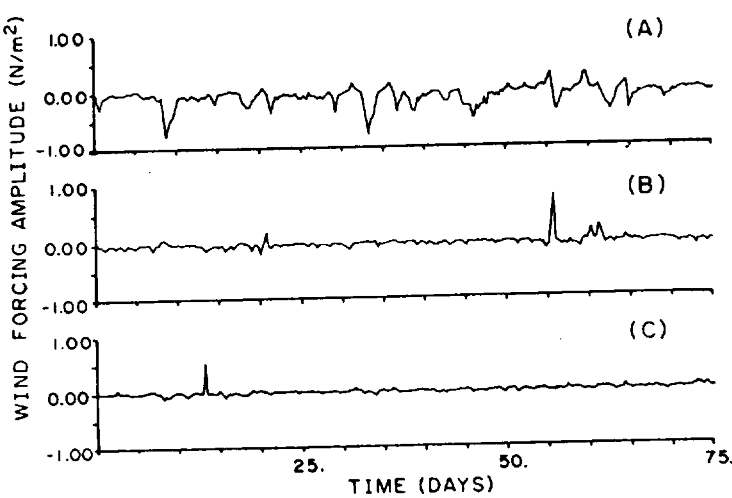

Fig. 4. Comparison of the wind stress curl terms by north-south component (B) and east-west component (C) with the wind stress term (A).

Numerical Method of Characteristics

If we limit the problem to a finite number of modes, 2j, (7) can be written as follows :

$$-\frac{\phi_{nt}}{C_n}+\phi_{ny}+a_{mn}\phi_n=G_n(y,t) \qquad (9)$$

where the forcing function $G_n(y, t)$ is defined as follows :

$$G_n(y,t)=\sum_{\substack{-j(j\neq 0)\\ \text{except } n}}^{j} a_{mn}\phi_m+b_{1n}\cdot\tau^y(-B_1)-b_{2n}\cdot\tau^y(B_2)$$

$$-\frac{1}{r_n}\int_{-B_1}^{B_2} F_n \cdot \left(\frac{d\tau^y}{dx}-\frac{d\tau^x}{dy}\right)dx \tag{10}$$

Along the characteristics defined by $Y_{nt}=-c_n(Y_n[t])$, (9) yields

$$\phi_{nt}-c_n a_{nn}\phi_n=-c_n G_n(Y_n[t],t) \tag{11}$$

Multiplying (11) by the integration factor as

$$E(t)=\exp\left[\int_0^t \{-c_n\}\{Y_n(t^*)\}a_{nn}\{Y_n(t^*)\}dt^*\right]$$

and integrating from $t-\delta t$ to t gives

$$\phi_n\{Y_n(t),t\}=\phi_n\{Y_n(t-\delta t),t-\delta t\}E(t-\delta t)/E(t) + \int_0^t [-c_n\{Y_n(t^*)\}G_n\{Y_n(t^*),t^*\}a_{nn}\{Y_n(t^*)\}dt] \tag{12}$$

where $Y_n(t^*)=Y_n(t)+\int_{t^*}^t c_n\{Y_n(t')\}dt'$.

Using the trapezoid rule to evaluate the integral in (12) gives the following difference formula relating $\phi_n\{Y_n(t),t\}=\phi_n\{Y_n(t-\delta t,t-\delta t)\}$.

$$\begin{aligned}\phi_n\{Y_n(t),t\}=&\phi_n\{Y_n(t-\delta t),t-\delta t\}.\\ &\times\exp[(\delta t/2)\cdot[c_n\{Y_n(t)\}\cdot a_{nn}\{Y_n(t)\}\\ &+c_n\{Y_n(t-\delta t)\}\cdot a_{nn}\{Y_n(t-\delta t)\}]]\\ &-(\delta t/2)\cdot c_n\{Y_n(t)\}\cdot G_n\{Y_n(t),t\}\\ &-(\delta t/2)\cdot c_n\{Y_n(t-\delta t)\}\cdot G_n\{Y_n(t-\delta t),r-\delta t\}\\ &\times\exp\left[(\delta t/2)\cdot[c_n\{Y_n(t)\}\cdot a_{nn}\{Y_n(t)\}\right.\\ &\left.+c_n\{Y_n(t-\delta t)\}\cdot a_{nn}\{Y_n(t-\delta t)\}]\right]\end{aligned} \tag{13}$$

where $Y_n(t-\delta t)=Y_n(t)+(\delta t/2)\cdot[c_n\{Y_n(t)\}+c_n\{Y_n(t-\delta t)\}]$.

Using the equation (10) enables (13) to be written as the matrix equation as follows :

$$\Gamma\cdot[I-(\delta t/2)K]=Q$$

where Γ is a row vector with the element $\phi_n(Y,t)$ and I is the identity matrix with j by j. The matrix K is given by

$$k_{mn}=\begin{cases}0 & \text{when } m=n\\ c_n\{Y_n(t)\}\cdot a_{mn} & \text{when } m\neq n\end{cases}$$

and Q is a row vector given by

$$\begin{aligned}q_n=&-(\delta t/2)c_n\{Y_n(t)\}[b_{1n}\tau^y(-B_1)-b_{2n}\tau^y(B_2)\\ &-\frac{1}{r_n}\int_{-B_1}^{B_2}F_n(\tau_x^y-\tau_y^x)dx]_{t=t}+\phi_n\{Y_n(t-\delta t),t-\\ &\delta t\}\times\exp\left[(\delta t/2)[c_n\{Y_n(t)\}a_{nn}\{Y_n(t)\}+c_n\right.\\ &\left.\{Y_n(t-\delta t)\}a_{nn}\{Y_n(t-\delta t)\}]\right]-(\delta t/2)\cdot c_n\{Y_n\\ &(t-\delta t)\}\cdot G_n\{Y_n(t-\delta t),t-\delta t\}\times\exp[(\delta t/2)\cdot\\ &\left[c_n\{Y_n(t)\}\cdot a_{nn}\{Y_n(t)\}+c_n\{Y_n(t-\delta t)\}\cdot a_{nn}\right.\\ &\left.\{Y_n(t-\delta t)\}]\right]\end{aligned} \tag{14}$$

With the restriction that $\varepsilon=(K\delta t/2)^2=(\delta t)^2 j(K_{max})^2/4 \ll 1$. We have within a small error ε

$$[I-(\delta t/2)K]^{-1}=[I+(\delta t/2)K].$$

Consequently, the solution for ϕ_n is

$$\Gamma=Q\cdot[I+(\delta t/2)K]. \tag{15}$$

In addition, δt must be small enough so that there is the same resolution in t as in y and aliasing is prevented.

Since, over a double shelf, there are two infinite wave sets propagating in opposite directions, we need two boundary conditions. Fig. 5 shows (A) a analytical solution and (B) a numerical solution of the first two modes over a double shelf (300~120km) channel of 500 km length shown in Fig. 6. Fig. 6 shows the model channel of straight coastlines in replacement of the

Yellow Sea, which is used in the previous application. The solid curves represent the time series of the wave function (ϕ_{-1}) propagating in the (+) y direction. So, its amplitude increases from the southern boundary (transection a at y=0km) where it is set to be zero to the northern boundary (transection b at y=500km). On the other hand, the dashed curves represent the time series of the wave function (ϕ_1) propagating in the (-) y direction. So, its amplitude increases from the northern boundary where it is set to be zero to the southern boundary. The analytical and numerical solutions show discrepancies only at the beginning. The initial difference is due to the fact that the analytical solution has only boundary conditions while the numerical solution has both boundary and initial conditions. Initially, sea level fluctuation is set to zero everywhere for the numerical solution. The duration over which the initial difference persists depends upon the phase speed c_n and is the time for the waves to travel the channel ($t=-y/c_n$ for waves propagating [+] y direction and $t=(500-y)/c_n$ for waves propagating [-] y direction). After the initial period, solutions are affected only by the boundary conditions and agree with each other, which implies that the numerical method works.

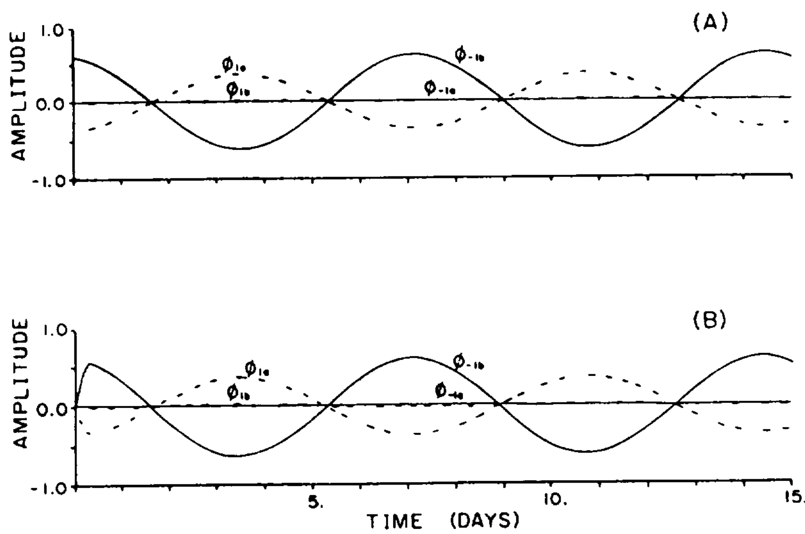

Fig. 5. (A) analytical and (B) numerical solitions of the first two wave functions : ϕ_1 (dashed lines) and ϕ_{-1} (solid lines). The amplitude is non dimensional. A northward (southward) propagating wave function ϕ_{-1} (ϕ_1) is amplified from the transection a (b) to the transection b (a) shown in figure 5. Numerical solutions are set to zero initially.

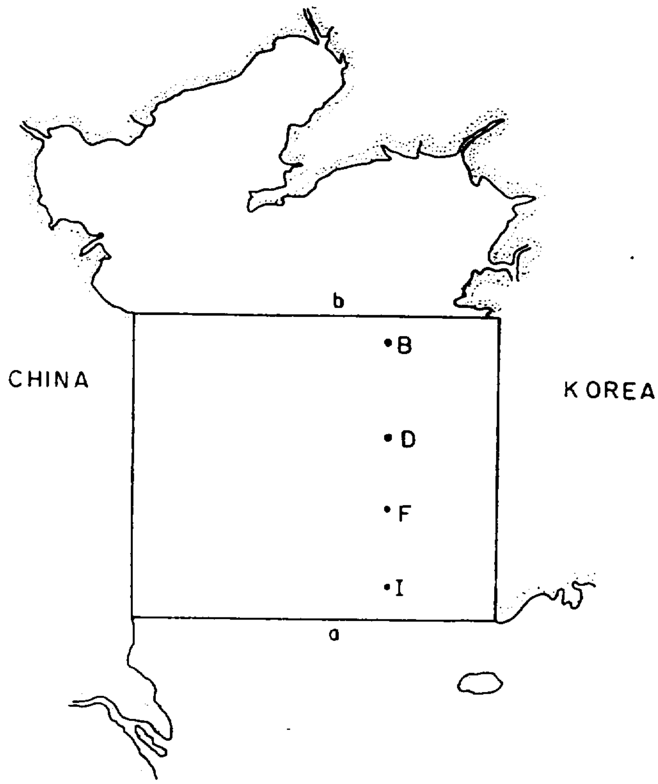

Fig. 6. A schematic representation of the insertion of the model channel in replacement of the Yellow Sea. The transections a and b mark the ends of the channel. B, D, F, and I, which lie along the model trough, are the locations of observation for the period of January-April, 1986.

Fig. 7 and 8 show, respectively, the sea level and alongshore velocity fluctuations along the Korea coast, calculated by a simple sinusoidal wind forcing $\tau^y=\tau_0 \cdot \cos(\ell y+\omega t)$. The values of τ_0, ℓ, and ω are, respectively, 10^{-1} Newton/m^2, 10^{-6} m^{-1}, and 10^{-5} sec^{-1}. As wave function, the amplitude of sea level and alongshore velocity increases from the southern boundary to the northern boundary along the Korea coast. The Kelvin wave mode makes a sunstantial contribution (about 80%) to sea level fluctuations. After the first 4 modes are included, there is no perceptible difference in the solutions. The sea levels calculated with the inclusion of the first 4 modes are thus a good approximation to the total solutions. It means that sea level fluctuations are due to mainly to the existence of Kelvin waves. However, Fig. 8 shows the Kelvin wave modes contribute almost nothing to alongshore velocity. Velocity is due mainly to the presence of continental shelf wave modes, among which the 1st modes contribute the most.

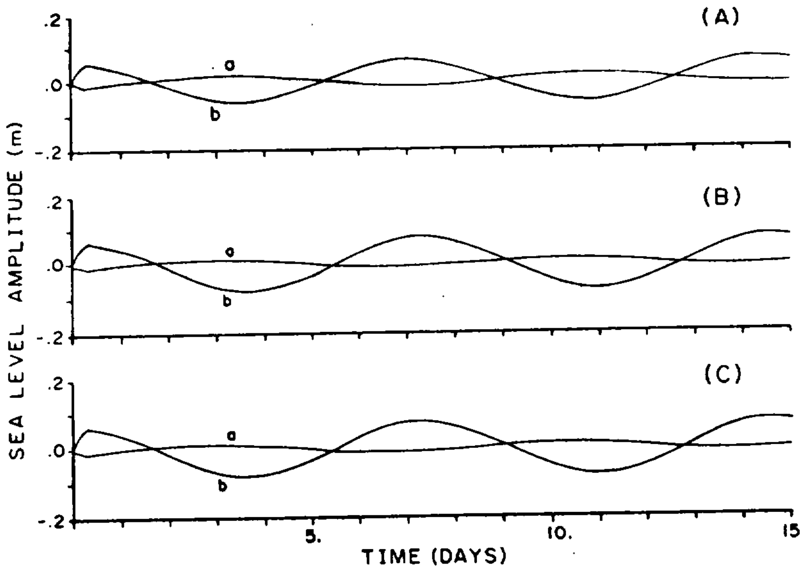

Fig. 7. Time series of calculated sea level fluctuations along Korea coast with inclusion of the first (A) 2, (B) 4, (C) 6 wave modes, driven by a simple sinusoidal wind forcing $\tau^y=\tau_0 \cdot \cos(\ell y+\omega t)$, where τ_0, ℓ, and ω are 10^{-1} Newton/m², $10^{-6}m^{-1}$, and 10^{-5} sec^{-1}, respectively.

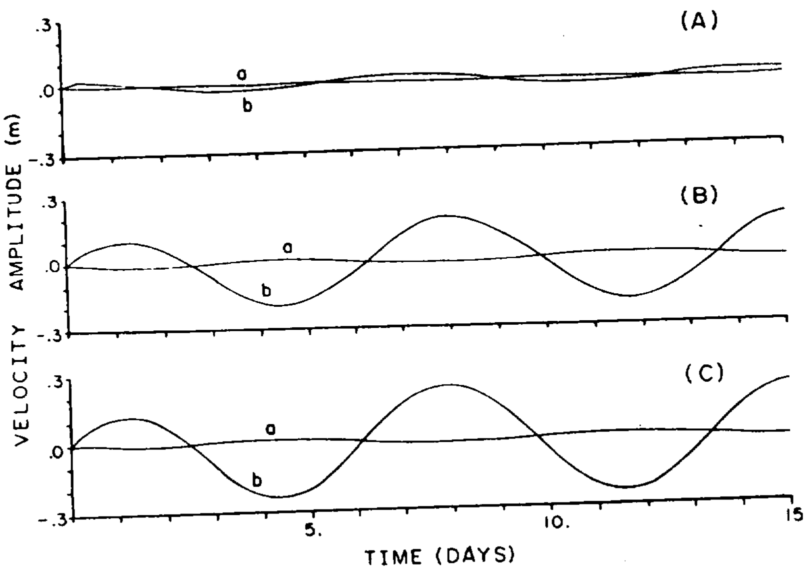

Fig. 8. Time series of calculated velocity fluctuations along Korea coast with inclusion of the first (A) 2, (B) 4, (C) 6 wave modes, driven by a simple sinusoidal wind forcing $\tau^y=\tau_0 \cdot \cos(\ell y+\omega t)$, where τ_0, ℓ, and ω are 10^{-1} Newton/m², $10^{-6}m^{-1}$, and 10^{-5} sec^{-1}, respectively.

Discussion and Conclusion

The first order wave equation over a double shelf has wind stresses on both castal boundaries and wind stress curl forcing across the shelf. However, the effect of wind stress curl can be neglected as a forcing of shelf waves in the Yellow Sea.

The decay distance of Kelvin waves is much greater than that of continental shelf waves. Therefore, Kelvin waves are transmitted nearly intact through the nortnern embayment while continental shelf waves are not. It suggests that the northern embayment of the Yellow Sea is necessary to be modelled for sea level hindcast, but not for velocity hindcast. Fig. 9 shows the comparison of (A) sea levels and (B) velocities, which are obtained with and without the modeled northern boundary region.

The numerical method of characteristics proceeds here in time increment to accomodate wave propagation of opposite directions and work fine.

The Kelvin wave makes a substantial contribution to sea level fluctuations. However, it contributes almost nothing to alongshore velocity. Velocity is due mainly to the presence of continental shelf waves, among which the lst modes contribute the most.

Although the wave model has been improved so far, it sould be improved more for better reproductions, specially in modelling the northern embayment. It is a future task, however, we understand that the long-period fluctuations of sea level and alongshore velocity in the Yellow Sea are basically due to the large scale ocean response driven by winds.

적 요

양향성 대륙붕에서 1차 파동방정식은 양 해안경계에서의 바람응력과, 대륙붕폭에 걸친 바람응력의 회전효과를 갖는다. 황해에서 바람응력 회전효과는 대륙붕파를 발생시키는 힘으로서 무시될 수 있다. 켈빈파는 대륙붕파보다 약화될 때까지의 거리가 매우 크기 때문에 황해 북쪽 만을 거의 약화되지 않고 통과할 수 있다. 파동특성을 따라 적분하는 수치방법은 반대방향으로 전파되는 파동을 수용하기 위해 조절되었다.

켈빈파는 해수면의 변화에 결정적인 역할을 한다. 그러나 켈빈파는 유속에는 거의 아무 영향도 주지 못하며 유속은 주로 대륙붕파에 의해 결정되며, 대륙붕파 중에서도 첫번째 모드가 대부분 결정한다.

References

Brink, K. H., 1983. Low-frequency free wave and wind-driven motions over a submarine bank. J. Phys. Oceanogr., 13, 103-116.

______, and J. S. Allen, 1978. On the effect of bottom friction on barotropic motion over the continental shelf. J. Phys. Oceanogr., 8, 919-922.

Clarke, A. J., and S. Van Gorder, 1986. A method for estimating wind-driven frictional time-dependent, stratified shelf and slope water flow. J. Phys. Oceanogr., 16, 1013-1028.

Gill, A. E., and E. H. Schumann, 1974, The generation of long shelf waves by the wind. J. Phys, Oceanogr., 19, 5, 612-625.

Hsueh, Y., 1988. Recent Current Observations in the eastern Yellow Sea. J. Geophys. Res., 93, 6875-6884.

_____, and I. C. Pang, 1989. Coastally trapped long waves in the Yellow Sea. J. Phys. Oceanogr., 19, 5, 612-625.

_____, and R. D. Romea, 1983. Wintertime winds and coastal sea-level fluctuations in the Northeat China Sea. Part 1 : Observations. j. Phys, Oceanogr., 13, 2091-2106.

_____, and J. H. Tinsman Ⅲ, 1987. A Comparison between Geostrophic and Observed Winds at a Japan Meteorological Agency buoy in the east China Sea. J. Oceanogr. Sce. Japan, 43, 251-257.

LeBlond, P. H., and L. A. Mysak, 1978. Waves in the Oceans. Elsevier, 602.

Louis, J. P., 1978. Low-frequency edge waves over a trenchridge topography adjoining a straight coastline. Geophys. Astrophy. Fluid Mech., 55, 113-127.

Mitchum, G. T., and A. J. Clarke, 1986. The frictional nearshore response to forcing by synoptic scale winds. J. Phys. Oceanogr., 16, 934-946.

Mysak, L. A., and P. H. LeBlond, and W. J. Emery, 1979. Trench waves. J. Phys, Oceanogr., 9, 1001-1013.

_____, 1980. Recent advances in shelf wave dynamics. Rev. Geophys. Space Phys., 18, 211-241.

_____, and A. J. Willmott, 1981. Forced trench waves. J. Phys. Oceanogr., 11, 1481-1502.

Pang, I. C., 1987. Theory of coastally trapped waves and its application to the Yellow Sea. Ph. D. Dissertation, Florida State University, 128pp.

_____, 1991. Coastally trapped waves over a double shelf topography (Ⅰ) : Free waves with exponential topography, Bill. Korean Fisher. Soc.. 24(6), 428-436.

_____, 1992. Coastally trapped waves over a double shelf topography (Ⅱ) : Free waves with linear topography, Bill. Korean Fisher. accepted.

_____ H. K. Rho, T. H. Kim, 1992. Seasonal Variations of Water Mass Distributions and their Causes in the Yellow Sea, the Eat China Sea, and the Adiacent Seas of Cheju Island. Bill. Korean Fisher. soc., 25(2), 151-162.

Taylor, G. I., 1921. Tidal Oscillations in gulfs and rectangular basins. Proc. Lond. Math. Soc., 2(20), 148-191.